

This document was prepared in conjunction with work accomplished under Contract No. DE-AC09-96SR18500 with the U.S. Department of Energy.

DISCLAIMER

This report was prepared as an account of work sponsored by an agency of the United States Government. Neither the United States Government nor any agency thereof, nor any of their employees, makes any warranty, express or implied, or assumes any legal liability or responsibility for the accuracy, completeness, or usefulness of any information, apparatus, product or process disclosed, or represents that its use would not infringe privately owned rights. Reference herein to any specific commercial product, process or service by trade name, trademark, manufacturer, or otherwise does not necessarily constitute or imply its endorsement, recommendation, or favoring by the United States Government or any agency thereof. The views and opinions of authors expressed herein do not necessarily state or reflect those of the United States Government or any agency thereof.

This report has been reproduced directly from the best available copy.

Available for sale to the public, in paper, from: U.S. Department of Commerce, National Technical Information Service, 5285 Port Royal Road, Springfield, VA 22161, phone: (800) 553-6847, fax: (703) 605-6900, email: orders@ntis.fedworld.gov online ordering: <http://www.ntis.gov/ordering.htm>

Available electronically at <http://www.doe.gov/bridge>

Available for a processing fee to U.S. Department of Energy and its contractors, in paper, from: U.S. Department of Energy, Office of Scientific and Technical Information, P.O. Box 62, Oak Ridge, TN 37831-0062, phone: (865) 576-8401, fax: (865) 576-5728, email: reports@adonis.osti.gov

Dynamic Analysis of 9975 Shipping Package without Overpack Subjected to 55-Foot Drop

Tsu-te Wu, Paul S. Blanton, and Allen C. Smith
Savannah River Technology Center
Westinghouse Savannah River Company
Aiken, South Carolina 29808
(803) 725-8201, tsu-te.wu@srs.gov

ABSTRACT

This paper discusses the evaluation of the dynamic response of a 9975 shipping package subjected to a load of 55-foot lateral drop without its overpack structure (fiberboard and drum). The fiberboard impact absorbent material and drum were removed so as to demonstrate a sufficiently large margin of safety for the package containment vessels when subjected to the above loading.

A nonlinear dynamic analysis was performed for a partial 9975 shipping package to evaluate the primary and secondary containment vessels structural response to a 55-foot drop. The structural integrity of the primary and secondary containment vessels are justified based on the analytical results in comparison with the stress criteria specified in the ASME Code, Section III, Appendix F for Level D service loads.

BACKGROUND

Crush testing of specimens cut from laminated cellulose fiberboard (Celotex™) used as the overpack of the 9975 shipping package showed that the dynamic responses vary with the orientation of the applied dynamic load [Smith, Vormelker, 2000]. These variations in the dynamic responses were attributed to the buckling of the glue layers used for bounding the fiberboard constituents [Gong, Wu, Smith, 2001]. The buckling of the glue layers in the overpack of a 9975 shipping package can generate an impulse load, which may amplify the dynamic response of the package subjected to a regulatory 30-foot drop. Therefore, the effect of glue layers on the dynamic response of the package need be accounted for. However, the buckling strength of a glue layer depends on its thickness, which is normally not in tight control and may vary widely in Celotex™ material. Consequently, a reliable analytical model of the overpack made of laminated cellulose fiberboard is difficult to develop.

As a bounding case of the dynamic responses of the 9975 containment vessels to a 30-foot drop, the finite-element analysis discussed in this paper was performed. In the present analysis, the cellulose fiberboard overpack was not considered to eliminate the uncertainty of the thickness of the glue layers. The finite-element model consisted of lead shielding, steel liner, secondary and primary containment vessels, 3013 outer can, spacer and metal content. For added

margin, the package was assumed to fall from the height of 55 feet.

ANALYSIS

The structural response of the 9975 shipping package to a 55-foot drop was simulated by performing nonlinear dynamic finite-element analysis with explicit time integration.

The ABAQUS/Explicit Computer Code, version 5.8 [HKS, 1998] was used to perform the computations. The finite-element meshes were generated using the MSC/PATRAN computer program [MacNeal-schwendler, 1999].

Input Data

The equipment evaluated is the 9975 shipping package. A sketch of the package cross section is shown in Figure 1. Figure 2 illustrates a solid cross section view of the analysis and the model components, i.e., lead shield, containment vessels and simulated contents.

The components, weight and geometric configuration of the 9975 shipping package are given in the Safety Analysis Report [1998].

The stress versus strain properties of the lead is shown in Figure 3. The stress versus strain curve of the 304L stainless steel containment vessels is shown in Figure 4. This data is also used for the lead shields steel liner. The material properties of the aluminum 3013-Spacer and lead shield lid are shown in Figure 5. Figure 6 shows the material properties for the 3013 container, 316L stainless steel.

The pressure-volumetric strain curve of a typical crushable foam material [Sauve et al, 1993] shown in Figure 7 was used to represent the material characteristics of the 9975 contents.

Table 1 summarizes the mechanical properties of the 9975 package components.

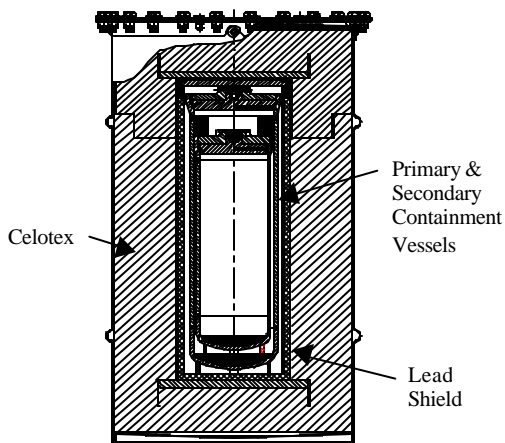


Figure 1. Configuration of 9975 Shipping Package

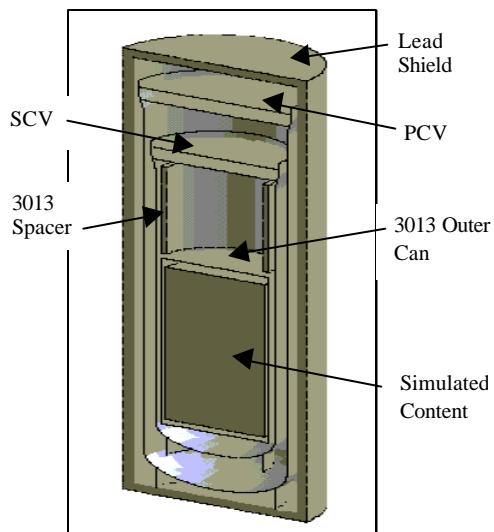


Figure 2. Solid Model used for 55-foot Dynamic Drop Analysis

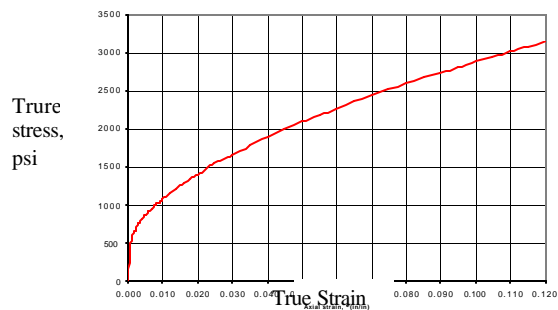


Figure 3 True Stress versus True Strain for Lead

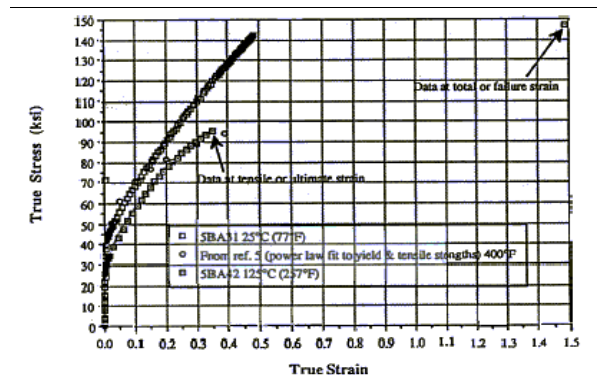


Figure 4. True Stress vs. True Strain Curve of 304L Stainless Steel

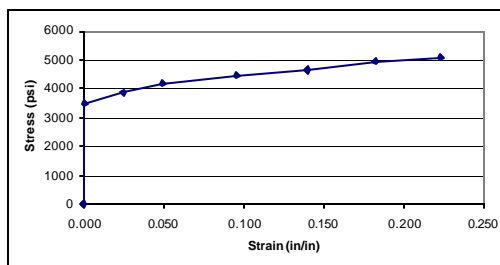


Figure 5. Stress vs. Strain Properties for Aluminum

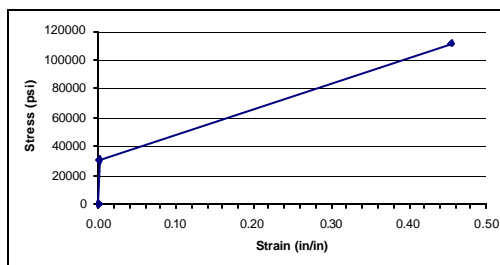


Figure 6. Stress vs Strain Properties for 316L Stainless Steel

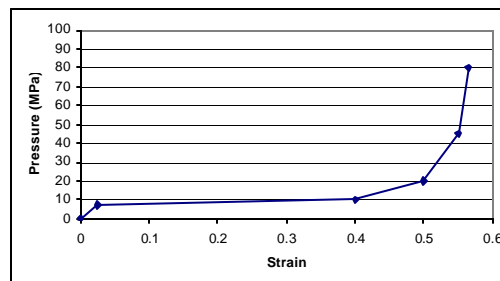


Figure 7. Foam Hardening Curve Pressure-volumetric strain curve in Sauve et al.

Table 1. Mechanical Properties of 9975 Package Components

| Component | Material | Modulus of Elasticity |
|---------------------------|----------------------|-----------------------|
| PCV, SCV, Tube | 304L Stainless Steel | 28.3E6 |
| 3013 Outer Can, Spacer | 316L Stainless Steel | 27.2E6 |
| Closure of Lead Shielding | Aluminum | 9.5E6 |
| Lead Shielding | Lead | 2.42E6 |
| Content | Foam (Assumed) | 18738.0 |

Table 1. Mechanical Properties of 9975 Package Components (continued)

| Component | Poisson's Ratio | Density (lb-sec ² /in ⁴) |
|---------------------------|-----------------|---|
| PCV, SCV, Tube | 0.3 | 7.324E-4 |
| 3013 Outer Can, Spacer | 0.3 | 7.391E-4 |
| Closure of Lead Shielding | 0.3 | 2.523E-4 |
| Lead Shielding Body | 0.43 | 0.00106 |
| Content | 0.0 | 0.0006464 |

Assumptions

The honeycomb spacers depicted in Figure 1, and not shown in Figure 2, were not included in the analysis because of the lateral drop orientation of the model. However, the containment vessels and content positions were defined by their physical geometry.

Contents completely fill the 3013 container. For purpose of this analysis it was assumed that the content behaves as crushable foam so that it will not resist the deflection of the PCV. However, the density of the content represents the actual weight of the content.

The primary and secondary containment vessel screwed closures and weldment were modeled as a single piece, i.e., the threaded closure is not modeled.

Finite-Element Model

The basic geometry of a 9975 shipping package is shown in Figure 1. The principal components are shown in the Figure 2 and are described in Table 2.

Since the arrangement of the package components are symmetric with respect to a plane containing the

axis of the package, only on-half of the package components; namely, one-half of the lead shielding assembly, SCV, PCV, 3013 outer container, spacer and content are included in the finite-element model.

The finite-element models of the SCV and PCV are comprised of three dimensional shell elements (Type S4R elements in the ABAQUS Computer Code). The lead shielding is modeled using 3D brick elements (Type C3D8R) three elements deep. Integral to the lead shield is the steel liner, which is modeled using 3D shell elements. The 3013 container and 3013-spacer are modeled with 3D shell elements and brick elements, respectively. The content is modeled using 3D brick elements. The target rigid floor is represented by a rigid element (Type R3D4). Figure 8 shows the overall finite-element model of the package.

Table 2. 9975 Package Components

| Item Number | Description | Material |
|-------------|---|---------------------------------|
| 1 | 5 inch Schdeule-40 Primary Containment Vessel (PCV) | 304L SST (ASME-SA312, 403, 479) |
| 2 | 6 inch Schedule-40 Secondary Containment Vessel (SCV) | 304L SST (ASME-SA312, 403, 479) |
| 3 | Shield | Lead (ASTM B-749) |
| 4 | Shield liner | 304 SST |
| 5 | 3013 container | 316 SST |
| 6 | Content | Crushable foam |
| 7 | 3013 spacer | Aluminum |
| 8 | Shield lid | Aluminum |

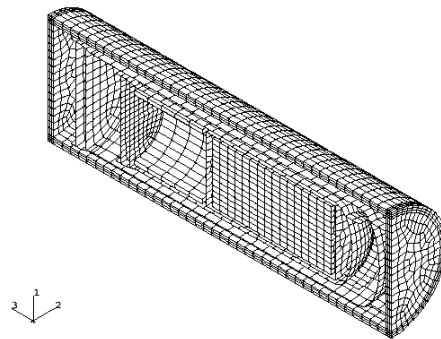


Figure 8. Finite-Element Model of 9975 Package

Applied Load and Initial Condition

The downward gravitational force of the falling package is represented by the gravitational load of 386.4 in/sec² in the negative “X” direction of the model.

The package is initially located near the target floor so that the initial velocity is equal to the velocity of the package after a 55-foot free fall in the negative x direction of the model. Therefore, the initial velocity can be calculated as follows.

$$V_0 = \sqrt{2gh} = \sqrt{2 \times 386.4 \frac{\text{in}}{\text{sec}^2} \times 12.0 \frac{\text{in}}{\text{ft}} \times 55 \text{ft}} = 714.2 \frac{\text{in}}{\text{sec}}$$

Boundary Conditions

Due to the symmetrical conditions of the geometry and loading, the following boundary conditions are applied at the nodes on the symmetrical plane along the axis of the package:

$$UX = 0; \quad RX = 0; \quad RZ = 0$$

Contact Conditions

The contact conditions between two surfaces are simulated by using the contact surfaces and the contact pair options and the penalty method available in ABAQUS Code.

DISCUSSION OF RESULTS

Stress Criteria in Accordance with ASME Code

The dynamic load associated with the 55-foot drop of a 9975 package is classified as a Level D Service Load defined in the ASME Code, Section III, Appendix F and the stress limits are defined as follows [ASME, 1998].

$$P_m \leq 0.7S_u$$

$$P_L \leq 0.9S_u$$

where P_m = General primary membrane stress intensity

P_L = Local primary membrane stress intensity

S_u = Ultimate strength of material

The maximum temperature under the normal condition of transport (NCT) is 313 °F and the ultimate strength of 304L stainless steel is 60.6 ksi

[Safety Analysis Report, 1998]. Thus, in terms of engineering stresses, the stress limits are as follows.

$$P_m \leq 0.7S_u = 0.7 \times 60.6 = 42.4 \text{ ksi} \quad \text{for temperature} = 313 \text{ }^\circ\text{F}$$

$$P_L \leq 0.9S_u = 0.9 \times 60.6 = 54.5 \text{ ksi} \quad \text{for temperature} = 313 \text{ }^\circ\text{F}$$

However, the results of the finite-element analysis are expressed in terms of true stresses and thus, the stress criteria should also be converted to true stresses. Since the engineering strain corresponding to the ultimate strength of 304L stainless steel is approximately equal to 0.35, the true ultimate stresses of the material is:

$$S_{tu} = S_u (\epsilon + 1) = 60.6(0.35 + 1) = 81.81 \text{ ksi} \quad \text{for temperature} = 313 \text{ }^\circ\text{F}$$

where,

S_{tu} = True ultimate stress of 304L stainless steel at 313 °F

ϵ = Engineering strain corresponding to ultimate strength

Consequently, the stress limits in terms of true stresses are:

$$P_m \leq 0.7S_{tu} = 0.7 \times 81.81 = 57.3 \text{ ksi} \quad \text{for temperature} = 313 \text{ }^\circ\text{F}$$

$$P_L \leq 0.9S_{tu} = 0.9 \times 81.81 = 73.6 \text{ ksi} \quad \text{for temperature} = 313 \text{ }^\circ\text{F}$$

The allowable limits of the stress intensities are summarized in Table 3.

Table 3. Allowable Limits of Stress Intensities

| Allowable Limits of Stress Intensity | | | |
|--------------------------------------|-------|-------------------|-------|
| Engineering Stress (ksi) | | True Stress (ksi) | |
| P_m | P_L | P_m | P_L |
| 42.4 | 54.5 | 57.3 | 73.6 |

Analytical Results

Deformed Shapes

Figure 9 shows the deformed shape of the full model. Figures 10 through 13 depict the deformed shapes of the PCV, SCV, lead shield liner and lead

shield, respectively, at the instant of 3 milliseconds after the package hits the target floor. Figures 10 and 11 indicate that the PCV bends slightly at knuckle of the bottom closure whereas the SCV deforms significantly both at the knuckle of the bottom closure and near the top closure. Figures 11 and 12 show that the lead liner and lead shield experience large permanent deformations.

Energy Plots

Figure 10 is the energy plots of the entire model. These plots show that the model loses its entire kinetic energy at approximately 3.5 milliseconds. Both plastic and internal energy (elastic plus plastic energy) reach the maximum values at approximately 3.5 milliseconds whereas elastic strain energy reaches its maximum value at approximately 2.5 milliseconds.

Velocity Plots

Figure 15 depicts the average velocities of the PCV head closure (designated by VPCVLID) and PCV bottom closure (designated by VPCVBOT). On the hand, Figure 16 depicts the average velocities of the SCV head closure (designated by VSCVLID) and SCV bottom closure (designated by VSCVBOT).

Calculated Values of Stresses Intensities

The stress components across the wall thickness should be used to calculate the General Primary Membrane Stress Intensities (P_m) and Local Primary Membrane Stress Intensities (P_L) in accordance with the ASME Code. However, for simplicity and conservatism, the maximum values of the von Mises stresses averaged across the vessel wall thickness, at the middle and the knuckle of the bottom closures of the PCV and SCV, which are approximately equal to the primary membrane stress intensities, are herein used to compare against the allowable stress limits for the general (P_m) and local (P_L) primary membrane stress intensities. Table 4 summarizes the stress results. Since these values are less than the allowable stress intensity and of 73.6 ksi for the local primary membrane stress intensity as given in Table 3., the structural integrity of the 9975 package subjected to a 55-foot drop is justified.

Calculated Values of Equivalent Plastic Strains

Furthermore, the maximum value of the equivalent plastic strain averaged across the wall thickness are equal to 0.11 and 0.15 for the PCV and SCV, respectively. These maximum equivalent plastic strains shown in Table 5 are less than the effective strain of 0.346, which corresponds to the ultimate strength of stainless steel 304L. Consequently, the PCV and SCV will not rupture after a 55-foot drop.

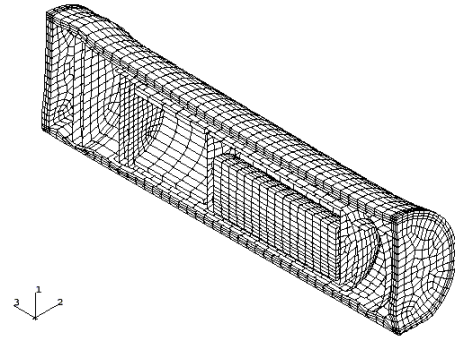


Figure 9. Deformed Shape of 9975 Package Model

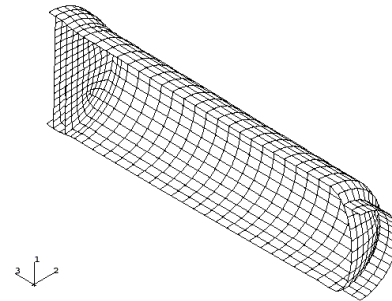


Figure 10. Deformed Shape of PCV

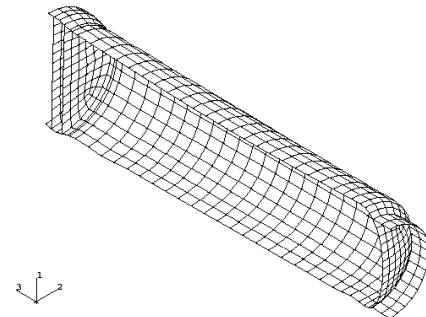


Figure 11. Deformed Shape of SCV

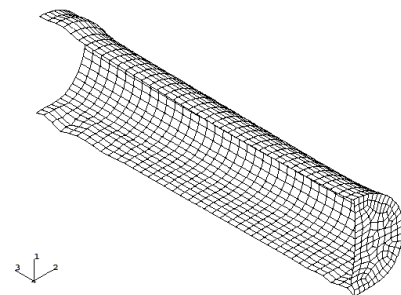


Figure 12. Deformed Shape of Lead Shield Liner

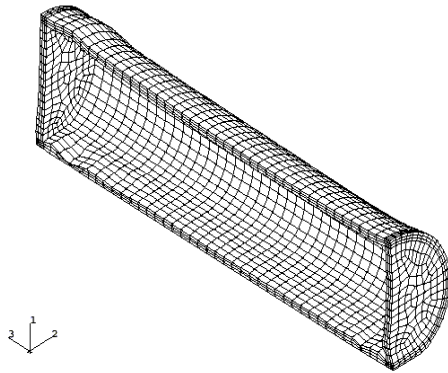


Figure 13. Deformed shape of Lead Shield

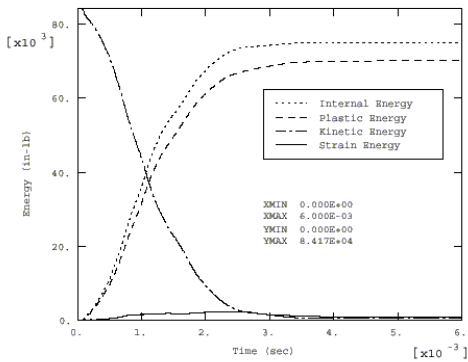


Figure 14. Energy Plots for the Entire Model

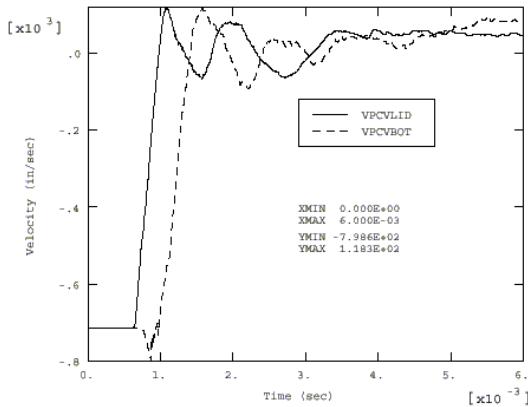


Figure 15 Averaged Velocities at PCV Top and Bottom Closures

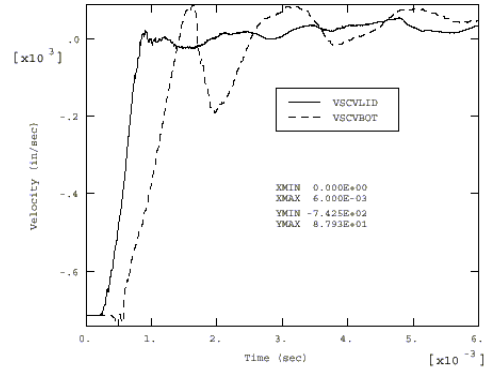


Figure 16. Averaged Velocities of SCV Top and Bottom Closures

Table 4. Calculated Maximum Values of Stress Intensities

| Component | Calculated Maximum Value of True von Mises Stress (ksi) | |
|-----------|---|-------|
| | P_m | P_L |
| PCV | 17.2 | 31.6 |
| SCV | 36.7 | 59.4 |

Figure 5. Calculated Maximum Values of Equivalent Plastic Strains

| Component | Calculated Maximum Value of Equivalent Plastic Strain | Strain Corresponding to Ultimate Strength |
|-----------|---|---|
| PCV | 0.11 | 0.35 |
| SCV | 0.15 | 0.35 |

REFERENCE

ASME, "1998 ASME Boiler and Pressure Vessel Code, Section III, Appendix F.

Gong, C., Wu, T. T. and Smith, A. C., 2001, Computational Parametric Analysis of Mechanical Behaviors of Celotex™ Implanted with Glue Plates, draft of 2001 PVP paper.

HKS, 1998, ABAQUS Theory manual, ABAQUS/Explicit User's Manual, version 5.8, Hibbit, Karlsson & Sorensen, In.

MacNeal-Schwendler Corp., MSC/PATRAN, Version 8.5, May 1999.

Smith, A. C., Vormelker, P. R., 2000, Celotex Structural Properties Tests (U), WSRC-TR-2000-000444, Technical Report, SRTC, WSRC, December 2000.

Safety Analysis Report – Packages 9972-9975
Packages (U), WSRC-SA-7, Revision 11,
Westinghouse Savannah River Company, Aiken SC
29803, December 2000.

Sauve, R. G., Morandin, G. D. and Nadeau, E.,
“Impact Simulation of Liquid-Filled Containers
Including Fluid-Structure Interaction,” *Journal of
Pressure Vessel Technology*, vol. 115, pp. 68-79,
1993.